Ultrasonic metamaterials with negative modulus

NICHOLAS FANG, DONGJUAN XI, JIANYI XU, MURALIDHAR AMBATI, WERAYUT SRITURAVANICH, CHENG SUN AND XIANG ZHANG*

Nano-scale Science and Engineering Center, 5130 Etcheverry Hall, University of California, Berkeley, California 94720-1740, USA
*e-mail: xiang@berkeley.edu

Published online: 30 April 2006; doi:10.1038/nmat1644

The emergence of artificially designed subwavelength electromagnetic materials, denoted metamaterials[1–10], has significantly broadened the range of material responses found in nature. However, the acoustic analogue to electromagnetic metamaterials has, so far, not been investigated. We report a new class of ultrasonic metamaterials consisting of an array of subwavelength Helmholtz resonators with designed acoustic inductance and capacitance. These materials have an effective dynamic modulus with negative values near the resonance frequency. As a result, these ultrasonic metamaterials can convey acoustic waves with a group velocity antiparallel to phase velocity, as observed experimentally. On the basis of homogenized-media theory, we calculated the dispersion and transmission, which agrees well with experiments near 30 kHz. As the negative dynamic modulus leads to a richness of surface states with very large wavevectors, this new class of acoustic metamaterials may offer interesting applications, such as acoustic negative refraction and superlensing below the diffraction limit.

A basic property of elastic material, the modulus of elasticity is defined as a measure of the resistance of the given material under applied force. Akin to electromagnetic response such as magnetic permeability, a material that exhibits negative modulus to acoustic excitation can consist of lumped-element inclusions. These structured materials may have many properties in common with the magnetic resonance: they can be described by an effective elastic modulus of the Lorentz form, provided that the structure is on a scale much smaller than the wavelength of excitation. This dynamic response is distinct from the so-called negative modulus originated from ferroelasticity, which requires a static energy that dictates material deformation[11], and in which a remarkable temperature dependence of the modulus is often accompanied by phase transition. Although the static elastic constant must be positive to maintain structural stability, an effective dynamic medium may possess a resonance-induced negative modulus, as demonstrated in sonic frequencies[12–14]. However, the focus so far has been limited to the emergence of bandgap[15] and applications for effective sound attenuation. Recently, studies on acoustic bandgap materials have shown refraction-like beam bending and refocusing[16], which requires the size of the building blocks to be close to the wavelength. A simulation predicted that high-index lenses can be made of subwavelength metamaterials[17]. Yet to the best of our knowledge, experimental realization of ultrasonic metamaterials as well as acoustic superlensing with engineered surface states still remains unexplored.

In this report, we present a new class of ultrasonic metamaterials that have strong dispersive characteristics of elastic modulus with subwavelength resonant structural units, which leads to a bulk mode propagating in the cluster of the units with group velocity antiparallel to the phase advancement. The building block of this ultrasonic metamaterial, the Helmholtz resonator, consists of a cavity of known volume with rigid walls and a small hole in one side (Fig. 1a). A pressure variation in the channel causes the plug of fluid in the hole to oscillate in and out, producing adiabatic compression and rarefaction of the liquid enclosed in the cavity. Such a resonator is analogous to an inductor–capacitor circuit (Fig. 1b)[18], with the enclosed cavity acting as the capacitor with capacitance $C \sim V/\rho c^2$, and the neck acting as the inductor ($L \sim \rho(L'/S)$), where V is the volume of the cavity, ρ is the density of the fluid, c is the sound speed in the fluid, L' is the effective length of the neck, and S is the cross-sectional area of the neck. Because the Helmholtz resonator does not use typical standing waves to create a resonance, the dimension of each element can be made much smaller than the acoustic wavelength (at 33 kHz, $\lambda = 4.4$ cm in water).

Owing to the fact that the periodicity is considerably smaller than the corresponding longitudinal wavelength in water ($d \sim \lambda/5$), the ultrasonic metamaterial behaves as a homogenized medium, and the built-in localized resonators give rise to a strong dispersion. Following the formalism of electromagnetic response in metamaterials[3,6], Fig. 1c shows that the combination of many Helmholtz resonators into a periodic array allows the material to behave as a medium with an effective modulus $E_{\text{eff}}(\omega)$ that can be expressed in the form,

$$E_{\text{eff}}^{-1}(\omega) = E_0^{-1}\left[1 - \frac{F\omega_0^2}{\omega^2 - \omega_0^2 + i\Gamma\omega}\right], \qquad (1)$$

where F is a geometrical factor, $\omega_0 \approx c\sqrt{S/L'V}$ is the resonant angular frequency, i indicates the imaginary component, and Γ is

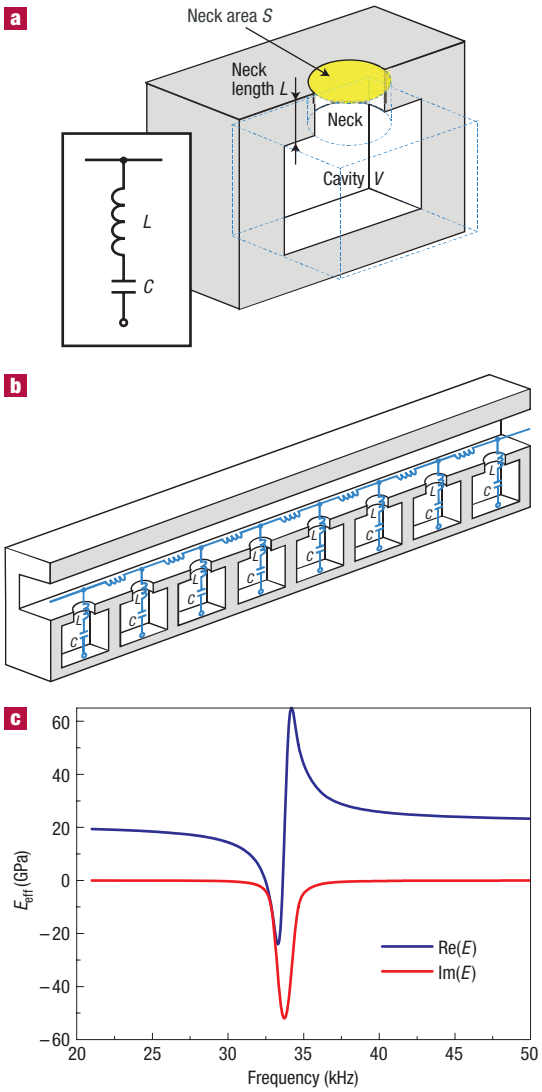

Figure 1 A new class of ultrasonic metamaterials consisting of arrays of subwavelength Helmholtz resonators. a, Schematic cross-sectional view of a Helmholtz resonator. The sample is made of aluminium, consisting of a rectangular cavity of $3.14 \times 4 \times 5$ mm, and a cylindrical neck 1-mm long and 1-mm in diameter. The cavity and neck are filled with water, and are connected at the same side to a square water duct with a 4×4 mm opening. The resonators are placed in a periodicity of 9.2 mm. The inset illustrates the analogy between a Helmholtz resonator and an inductor–capacitor circuit, showing the fluidic inductance due to the neck, and the acoustic capacitance due to the cavity. **b**, Illustration of periodical daisy-chained Helmholtz resonators, giving rise to a complex acoustic admittance in the fluidic network. **c**, The calculated effective bulk modulus in the above one-dimensional subwavelength Helmholtz resonators. As the structures are considerably smaller than the wavelength at the frequency range, the medium can be homogenized with an effective modulus as described by equation (1).

the dissipation loss in the resonating Helmholtz elements. Note that in Fig. 1c, the imaginary part of the modulus has a negative sign because the acoustic analogue of permeability corresponds to $1/E$. This frequency-dependent response is essential to the negative modulus over a range of frequencies. At frequencies near resonance, the induced displacement in the neck becomes very large, as is typical in resonance phenomena. The large response represents accumulation of energy over many cycles, such that a considerable amount of energy is stored in the resonator relative to the driving field. This stored energy is significant to maintain the sequence of displacement near resonance even when the excitation field changes the sign. That is, as the frequency of the driving pressure field is swept through the resonance, the instantaneous displacement of the mass centre in the unit cell flips from in-phase to out-of-phase with the driving field, and the material shows a negative response. Similarly, a polariton effect is also observed in the electromagnetic response of metamaterials, where a negative permittivity or permeability (generally on the higher frequency side of the resonance) implies a purely imaginary wavevector in the bulk medium. Here, we implement this idea in the context of elastic composites at ultrasonic frequencies. By varying the size and geometry of the structural unit, we can tune the effective elastic moduli to negative values at desired frequency ranges.

To characterize the unique propagation properties of acoustic waves in this ultrasonic metamaterial made of Helmholtz resonators, we conducted a set of underwater ultrasonic-transmission experiments on one-dimensional daisy-chained samples (see Fig. 2a and the Methods section). An appreciable range of negative group delay time is found at the anomalous dispersion region of the one-dimensional ultrasonic metamaterial (Fig. 2b); this negative group delay time means that a sound pulse propagating along the channel of ultrasonic metamaterials emerges downstream significantly earlier than if it had propagated the same distance in a water channel, so the peak of the pulse seems to leave the duct before entering it. The negative group velocity observed is a clear indicator of the negative modulus of the ultrasonic metamaterials. This is because the product of wavevector $\mathbf{k}$ and Poynting vector $\mathbf{S}$ characterizes the dissipation of energy flux of acoustic waves, and it is described by

$$\mathbf{k}\cdot\mathbf{S} = (\omega/2)\left[\rho|\mathbf{v}|^2 + (\partial(\omega/E)/\partial\omega)|p|^2\right],$$

where ω describes the angular frequency, $|v|$ is the amplitude of the maximum flow velocity, and $|p|$ is the maximum pressure difference in the channel. When the real component of the second term, $\mathrm{Re}[(\partial/\partial\omega)(\omega/E)]$, is negative and sufficiently large, as we can observe in the region of negative modulus within a narrow frequency range of 30–35 kHz (Fig. 1c), $\mathrm{Re}(\mathbf{k}\cdot\mathbf{S}) < 0$, and the group velocity that follows the direction of the Poynting vector is antiparallel to the phase propagation direction indicated by $\mathbf{k}$. The supersonic-pulse propagation observed obeys causality, being a direct consequence of classical interference on the re-emission sequences of the coupled resonators in an anomalous dispersion region[19]. When the pulse train reaches the daisy-chained resonators, the first few cycles are not able to fully excite the resonators to the maximum amplitude. The excess energy is flowing through the channel, forming an early peak of the envelope of the pulse train downstream. When the rest of the pulses enter the channels they are absorbed more efficiently, pumping the resonators to maximum resonance, leading to a peak upstream. We also observed that the pulse train upstream is less distorted from the original form, and the power peaks near the middle of the burst. A control experiment was carried out using the same configuration without resonators, and, as expected, it shows no negative delay time (Fig. 2b). The occurrence of negative group velocity is also predicted by our theoretical calculation of transit time on a stratified medium, assuming a bulk modulus of the form given by equation (1), as shown in Fig. 2b.

Integration over the reciprocal group velocity as a function of frequency yields the dispersion curve of the ultrasonic metamaterial, as shown in Fig. 2c. For comparison, we also plotted the theoretical lossless dispersion curve (see the Supplementary Information) in the same periodical array of daisy-chained

resonators. Theory on the lossless resonators predicts that a full bandgap opens up between 32 and 34 kHz, whereas away from this dip the dispersion behaves linearly. However, experimental data show that possible propagation modes can exist in the bandgap with a back-bending of the dispersion curve, which suggests an antiparallel relation between group and phase velocities. This is a direct result of the loss in the system, such as the friction between the solid wall and the fluid, although viscous dissipation is secondary. When ultrasonic metamaterials approach resonance, the complex modulus $E = -|\mathrm{Re}(E)| + i\mathrm{Im}(E) = -\alpha - i\beta$ is expected in the spectral dip as a result of friction dissipation ($\alpha, \beta > 0$ as shown in Fig. 1c), where $\mathrm{Im}(E)$ indicates the imaginary part, and α, β are parameters corresponding to the real and imaginary parts of the complex modulus. It is straightforward to write the propagation constant in the system as $k = (-\alpha + i\beta)^{1/2}\omega\sqrt{\rho/(\alpha^2+\beta^2)}$, with a small real component

$$\mathrm{Re}(k) = -\frac{\omega}{2}\sqrt{\frac{\rho}{\alpha^2+\beta^2}}\cdot\left\{\sqrt{\alpha^2+\beta^2}-\alpha\right\}^{1/2}$$

characterizing a propagating mode in the bandgap, whereas the imaginary part

$$\mathrm{Im}(k) = +\frac{\omega}{2}\sqrt{\frac{\rho}{\alpha^2+\beta^2}}\cdot\left\{\sqrt{\alpha^2+\beta^2}+\alpha\right\}^{1/2}$$

describes the decaying length of the pulse. The dispersion of these complex wavevectors can be well captured in our experiment by sweeping in real frequencies. Taking into account a small propagating component as an effect of resonant re-emission in parallel to the dominant tunnelling process in the transmission dip, the dispersion relationship can be accurately characterized in our experimental results (Fig. 2c). In addition, as frequency increases above the band edge, the loss (β) increases leading to the reduction of the amplitude of the real wavevector $\mathrm{Re}(k)$, resulting in the back-bending of the dispersion curve observed in Fig. 2c. This is an intrinsic feature associated with dissipation in the resonators. A similar result was considered as a pure mathematical curiosity in the optical excitation of polaritons[20], until Arakawa[21] reported experimental data on a surface plasmon obtained with a fixed frequency and sweeping angle of incidence. The back-bending observed in our experiment clearly demonstrates that in the frequency region where polaritonic states dominate, the ultrasonic metamaterials convey acoustic waves with a group velocity antiparallel to phase advancement.

For comparison, a control experiment is carried out with a control sample that has the same configuration, but without resonators in the duct. As expected, the group tunnelling time in the control sample is close to constant (Fig. 2b). This is because the dimension of the channel set up a cut-off frequency of 200 kHz for the transverse modes, as a result, only longitudinal plane waves at a frequency of 20–50 kHz can propagate in the channel and be measured.

To further understand the dynamic negative modulus of the ultrasonic metamaterials, the transmission loss is also measured, as shown in Fig. 3. We observed an attenuation band located from 31 to 35 kHz (Fig. 3). This is in good agreement with the designed resonance of Helmholtz resonators at 32.5 kHz. We also carried out a control experiment, which shows no sign of sharp absorption. The monotonic increase of the transmission in the control sample is attributed to the increasing ratio of the channel diameter to the acoustic wavelength in water. Substituting the frequency-dependent modulus shown in Fig. 1c into the Fresnel formula of stratified media, we plot the calculated transmission of the 55-cm slab ultrasonic metamaterial as a function of

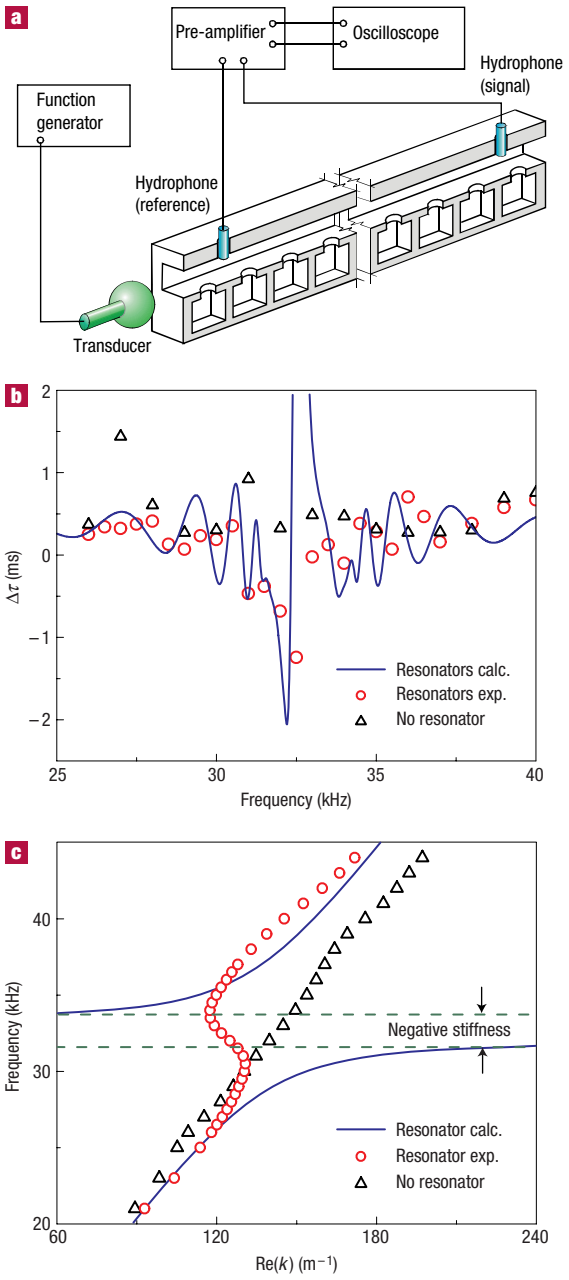

Figure 2 Ultrasonic experiments demonstrating the negative dynamic modulus of the acoustic metamaterials near 32 kHz. a, Illustration of the setup of the ultrasonic transmission experiment. A burst of monotonic signal with a width of 10 periods was used to drive the transducer as an underwater sound source towards one end of the channel, and two needle-sized hydrophones detected the ultrasonic signals inside the channel. **b**, Measured and calculated group transit delay time ($\Delta\tau$) as a function of frequency from upstream to downstream detectors; **c**, Measured and calculated dispersion of ultrasonic metamaterial. In **b** and **c** the red circles represent data measured from the periodical array of Helmholtz resonators in the duct, the black triangles represent the data in the duct without Helmholtz resonators, and the blue solid line is calculated using a sum of lossless Bloch waves[29].

frequency, together with experimental transmission data. The loss term ($\Gamma = 2\pi \times 400$ Hz) is determined empirically by fitting the calculated transmission data along the edges of the experimental

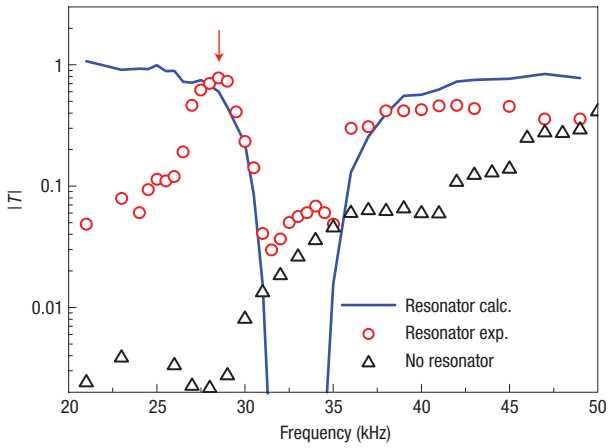

Figure 3 Measured and calculated transmission (amplitude ratio) as a function of frequency between upstream and downstream detectors. The red arrow indicates a Fano-like asymmetric peak, attributed to the existence of non-resonant paths in the channel. The deviation from theoretical prediction at the absorption band is probably due to the sensitivity of the hydrophones in the experiment.

spectral dip. The good agreement between theory and experiment indicates that the dynamic negative modulus in the ultrasonic metamaterials shown in Fig. 3 is responsible for the transmission dip observed experimentally.

We also found Fano-like asymmetric transmission peak profiles at the onset of resonance, due to the fact that a portion of the waves can travel in a non-resonant path. The interference of both resonant and non-resonant paths results in an asymmetric profile at the proximity of resonance frequency (25–30 kHz), similar to the observations in the optical regime[22]. According to ref. 22, the Fano-like asymmetric transmission peak below resonance suggests that the phase difference of the waves coupled to the resonators, and those travelling from the background, have a phase difference close to π. This phenomenon is in agreement with the backward wave propagation observed. These unique features of the measured dispersion characteristics and the transmission profile clearly indicate the important role of dynamic negative modulus in ultrasonic metamaterials.

Although this experiment studies sound propagation in one-dimensional ultrasonic metamaterials, the extension of this work to two or three dimensions promises novel applications in imaging. In conventional acoustic bandgap materials[23–25], the acoustic waves are strongly diffracted when the wavelength is close to the size of the scatterers. In contrast, the ultrasonic metamaterials act as a homogenized medium to the acoustic excitation because their lattice constants are much smaller than the wavelength. Therefore, ultrasonic metamaterials offer a new opportunity in making compact and tunable acoustical devices, such as small footprint sonar and medical ultrasonic scanners. In addition, negative modulus can introduce collective surface oscillations. These resonant surface modes have very large wavevectors at the interface between two materials of opposite signs of modulus, similar to the surface plasmon on the metal–dielectric interface[26]. The emergence of these surface states allows the coupling between the evanescent spectrum from a subwavelength object into the ultrasonic metamaterials with strong enhancement[9,27]. This strong evanescent enhancement could compensate evanescent decay in the free space, leading to a potential acoustic superlens that produces images well below the diffraction limit, analogous to electromagnetic superlensing[27,28]. Instead, the loss of the system, mostly attributed to the viscous dissipation of the fluid and the wall, would eventually limit the imaging resolution, in a similar fashion to their electromagnetic counterparts. The artificial ultrasonic metamaterials with designed negative modulus and dispersion open a new horizon in acoustic imaging below the diffraction limit.

METHODS

SAMPLE FABRICATION

Both the duct and the Helmholtz resonators were made of aluminium. The cavity and neck were engraved by mechanical drilling on metallic slabs; then they were assembled together with other pieces to form an enclosed tube with a 4×4-mm channel cross-section. This channel dimension was designed to ensure that only a plane wave longitudinal mode was allowed to propagate below the frequency of 200 kHz.

EXPERIMENTAL SETUP AND DATA ACQUISITION

Ultrasonic transmission was measured using a homemade aluminium duct immersed in water (Fig. 2a). The sound source, an underwater transducer (model ITC-1042, International Transducers Corporation), was mounted at one end of the aluminium duct. A waveform generator (model DS345, Stanford Research Systems) was used to drive the underwater transducer. The source generated a burst of sine waves with a width of 10 periods. The sample of the daisy-chained resonators was embedded in the duct, with two needle-sized hydrophone detectors inserted half way into the duct at the top side of the ultrasonic metamaterial, and separated by 55 cm (corresponding to 59 resonators). The signal transmitted upstream and downstream was measured by Endevco 6507C needle-sized hydrophones (dynamic range 23 dB), amplified by the Endevco 136 DC amplifier, and captured using a digital oscilloscope (Agilent 54624A), then downloaded to a computer for post-processing and analysis. Post-processing was used to filter the central frequency to leverage the stray noise and corresponding distortion of waveforms. Transmission was measured as a function of frequency from 20 to 60 kHz for the daisy-chained resonators. The signal was averaged every 512 sampling runs for the purpose of noise reduction. The transit time and maximum amplitude of the pulses were obtained from the signals measured from the detectors placed upstream and downstream, and the group tunnelling time (Fig. 2b) was determined by measuring the difference between the peak position of upstream and downstream acoustic signals.

We note the limitations on our experimental technique that prevent us from probing the group transit time corresponding to the extremes of the resonant modulus band. When the effective modulus reaches the positive or negative extrema, the group velocity in the metamaterial becomes very low. This implies that it takes a very long time for the wave train to completely travel through the sample, and it is difficult to separate the signal from the background reflections. Meanwhile, the time span of the original burst is of the order of 3 ms, corresponding to a frequency resolution $\Delta f \sim 1/(2\Delta\tau) = 0.16$ kHz. Thus, we are unable to unambiguously determine very small or very large propagation constants that change dramatically in the frequency region from about 27 to 32 kHz, which would correspond to an imaginary wavenumber rather than positive as measured. This limitation might be eased by the use of a longer burst and reduced background noise.

Received 9 January 2006; accepted 8 March 2006; published 30 April 2006.

References

1. Veselago, V. G. Electrodynamics of substances with simultaneously negative values of sigma and mu. *Sov. Phys. Uspekhi-USSR* **10,** 509–514 (1968).
2. Pendry, J. B., Holden, A. J., Stewart, W. J. & Youngs, I. Extremely low frequency plasmons in metallic mesostructures. *Phys. Rev. Lett.* **76,** 4773–4776 (1996).
3. Pendry, J. B., Holden, A. J., Robbins, D. J. & Stewart, W. J. Magnetism from conductors and enhanced nonlinear phenomena. *IEEE Trans. Microw. Theory Tech.* **47,** 2075–2084 (1999).
4. Smith, D. R., Padilla, W. J., Vier, D. C., Nemat-Nasser, S. C. & Schultz, S. Composite medium with simultaneously negative permeability and permittivity. *Phys. Rev. Lett.* **84,** 4184–4187 (2000).
5. Wiltshire, M. C. K. *et al.* Microstructured magnetic materials for RF flux guides in magnetic resonance imaging. *Science* **291,** 849–851 (2001).
6. Iyer, A. K., Kremer, P. C. & Eleftheriades, G. V. Experimental and theoretical verification of focusing in a large, periodically loaded transmission line negative refractive index metamaterial. *Opt. Express* **11,** 696–708 (2003).
7. Yen, T. J. *et al.* Terahertz magnetic response from artificial materials. *Science* **303,** 1494–1496 (2004).
8. Linden, S. *et al.* Magnetic response of metamaterials at 100 terahertz. *Science* **306,** 1351–1353 (2004).
9. Pendry, J. B. Negative refraction makes a perfect lens. *Phys. Rev. Lett.* **85,** 3966–3969 (2000).
10. Ziolkowski, R. W. & Heyman, E. Wave propagation in media having negative permittivity and permeability. *Phys. Rev. E* **64,** 056625 (2001).

11. Lakes, R. S., Lee, T., Bersie, A. & Wang, Y. C. Extreme damping in composite materials with negative-stiffness inclusions. *Nature* **410,** 565–567 (2001).
12. Liu, Z. Y. *et al.* Locally resonant sonic materials. *Science* **289,** 1734–1736 (2000).
13. Goffaux, C. *et al.* Evidence of Fano-like interference phenomena in locally resonant materials. *Phys. Rev. Lett.* **88,** 225502 (2002).
14. Li, J. & Chan, C. T. Double-negative acoustic metamaterial. *Phys. Rev. E* **70,** 055602 (2004).
15. Sigalas, M. M. *et al.* Classical vibrational modes in phononic lattices: theory and experiment. *Z. Kristallogr.* **220,** 765–809 (2005).
16. Yang, S. X. *et al.* Focusing of sound in a 3D phononic crystal. *Phys. Rev. Lett.* **93,** 024301 (2004).
17. Hu, X. H., Chan, C. T. & Zi, J. Two-dimensional sonic crystals with Helmholtz resonators. *Phys. Rev. E* **71,** 055601R (2005).
18. Kinsler, L. E. *Fundamentals of Acoustics* 3rd edn (Wiley, New York, 1982).
19. Yang, S. X. *et al.* Ultrasound tunneling through 3D phononic crystals. *Phys. Rev. Lett.* **88,** 104301 (2002).
20. Halevi, P. in *Electromagnetic Surface Modes* (ed. Boardman, A. D.) Ch. 7 (Wiley, New York, 1982).
21. Arakawa, E. T., Williams, M. W., Hamm, R. N. & Ritchie, R. H. Effect of damping on surface plasmon dispersion. *Phys. Rev. Lett.* **31,** 1127–1129 (1973).
22. Lee, H. T. & Poon, A. W. Fano resonances in prism-coupled square micropillars. *Opt. Lett.* **29,** 5–7 (2004).
23. Kushwaha, M. S., Halevi, P., Dobrzynski, L. & Djafarirouhani, B. Acoustic band-structure of periodic elastic composites. *Phys. Rev. Lett.* **71,** 2022–2025 (1993).
24. de Espinosa, F. R. M., Jimenez, E. & Torres, M. Ultrasonic band gap in a periodic two-dimensional composite. *Phys. Rev. Lett.* **80,** 1208–1211 (1998).
25. Martinez-Sala, R. *et al.* Sound-attenuation by sculpture. *Nature* **378,** 241 (1995).
26. Pendry, J. B., Martin-Moreno, L. & Garcia-Vidal, F. J. Mimicking surface plasmons with structured surfaces. *Science* **305,** 847–848 (2004).
27. Fang, N., Lee, H., Sun, C. & Zhang, X. Sub-diffraction-limited optical imaging with a silver superlens. *Science* **308,** 534–537 (2005).
28. Cubukcu, E., Aydin, K., Ozbay, E., Foteinopolou, S. & Soukoulis, C. M. Subwavelength resolution in a two-dimensional photonic-crystal-based superlens. *Phys. Rev. Lett.* **91,** 207401 (2003).
29. Sugimoto, N. & Horioka, T. Dispersion characteristics of sound-waves in a tunnel with an array of Helmholtz resonators. *J. Acoust. Soc. Am.* **97,** 1446–1459 (1995).

Acknowledgements

This research was supported by the ONR/DARPA Multidisciplinary University Research Initiative (MURI) (grant N00014-01-1-0803) and the NSF Nanoscale Science and Engineering Center (NSEC) (grant DMI-0327077). The authors also thank A. Mal at the University of California, Los Angeles for allowing us to use his ultrasonic measurement facilities.
Correspondence and requests for materials should be addressed to X.Z.
Supplementary Information accompanies this paper on www.nature.com/naturematerials.

Competing financial interests

The authors declare that they have no competing financial interests.